

Computer studies of spin and energy transport in one-dimensional Heisenberg magnets*

N. A. Lurie[†]

Brookhaven National Laboratory, Upton, New York 11973
Brandeis University, Waltham, Massachusetts 02154

D. L. Huber[‡]

Brookhaven National Laboratory, Upton, New York 11973

M. Blume

Brookhaven National Laboratory, Upton, New York 11973
State University of New York, Stony Brook, New York 11790

(Received 7 August 1973)

We have studied the dynamics of the classical Heisenberg chain at finite and infinite temperatures by computer simulation of an array of 4000 spins. The evaluation of the spin-spin and energy-energy wave-vector- and time-dependent correlation functions out to time $10J^{-1}$ made it possible to determine the spin and energy diffusion constants. At infinite temperature we find $D_S = (1.33 \pm 0.10)JSa^2$ and $D_E = (3 \pm 1)JSa^2$. Values of D_S have also been determined, with less precision, for ferromagnetic and antiferromagnetic interactions at temperatures $k_B T/|J| = 1.0$ and 0.5 . Our results are compared with various theoretical estimates. In addition, we calculate the time-dependent spin and energy self-correlation functions.

I. INTRODUCTION

The hydrodynamic formalism has often been a successful starting point for the description of the response of many-body systems to low-frequency-long-wavelength disturbances.¹ Originally developed for classical liquids,² it has been applied in recent years to the characterization of various transport phenomena in solids. The essential feature of these theories is the identification of a set of densities, e.g., mass density, energy density, momentum density, whose spatial integrals are constants of the motion. Differential equations, the hydrodynamic equations, are developed to describe the temporal evolution of these densities. The normal-mode solutions to these equations are typically characterized by velocities of propagation and damping constants. The velocities are expressed in terms of parameters characterizing the thermodynamic state of the system. The damping constants, on the other hand, are combinations of phenomenological parameters.

The success of the hydrodynamic description has spurred attempts to derive the equations using a microscopic formalism.^{3,4} In such a program one obtains explicit expressions for the damping constants in terms of the microscopic properties of the system. In addition, information is gained about the range of validity of the hydrodynamic theory.

In the case of magnetic insulators the appropriateness of a hydrodynamic description of the transport of excitation in the magnetic lattice was apparently first pointed out by Bloembergen.⁵ The essence of his argument is that in systems where

the dominant spin-spin interaction is of the Heisenberg form

$$\sum_{(i,j)} \frac{1}{2} J_{ij} \vec{S}_i \cdot \vec{S}_j,$$

the total spin, $\sum_j \vec{S}_j$, is a constant of the motion. Assuming no long-range order, the fluctuations in the total spin, $\vec{S}(\vec{q}, t) = \sum_j e^{i\vec{q}\cdot\vec{r}_j} \vec{S}_j(t)$, in the hydrodynamic region should be governed by the diffusion equation

$$\frac{\partial \vec{S}(\vec{q}, t)}{\partial t} = -D_S q^2 \vec{S}(\vec{q}, t), \quad (1.1)$$

where D_S is the spin-diffusion constant. In addition, the energy density $E(\vec{q}, t)$ obeys a similar equation,

$$\frac{\partial E(\vec{q}, t)}{\partial t} = -D_E q^2 E(\vec{q}, t), \quad (1.2)$$

in which D_E is the energy (or thermal) diffusion constant. It is important to note that the particularly simple form for the hydrodynamic equations, (1.1) and (1.2), is a direct consequence of the assumption that there is no long-range order in the system. When this is not the case there is a coupling between the spin and energy densities as well as propagating modes (i.e., spin waves).^{6,7}

Experimental information about the magnitude and temperature dependence of D_S and D_E is rather limited. Inelastic neutron scattering, in principle, provides the most direct information about the spin-diffusion constant, since the hydrodynamic formalism leads to an expression for the cross section which is proportional to $D_S q^2 / [\omega^2 + (D_S q^2)^2]$ for mo-

momentum transfer \vec{q} and energy transfer ω ($\hbar=1$). However, the measurements are hampered by finite resolution, which complicates the identification of the limiting behavior of the cross section as \vec{q} and ω approach zero. To our knowledge the only experimental information about D_E has come from nuclear-magnetic-resonance studies in ^3He .⁸

In this paper we report studies of spin and energy transport in one-dimensional Heisenberg magnets. The information is obtained by solving the equations of motion of a ring of 4000 spins governed by the Hamiltonian

$$H = -J \sum_{i=1}^{N-1} \vec{S}_i \cdot \vec{S}_{i+1} - J \vec{S}_N \cdot \vec{S}_1, \quad (1.3)$$

where $N=4000$. The spins are treated as classical variables whose time evolution is determined by the equation of motion

$$\frac{d\vec{S}_i}{dt} = J[\vec{S}_i \times (\vec{S}_{i+1} + \vec{S}_{i-1})], \quad (1.4)$$

where $\hbar=1$. As will be discussed below, initial values for the \vec{S}_i are chosen corresponding to the system being in thermal equilibrium. Correlation functions $\langle S(-q, 0)S(q, t) \rangle$ and $\langle E(-q, 0)E(q, t) \rangle$ are computed, and from the asymptotic behavior of these functions, estimates are obtained for D_S and D_E .

Previous computer studies of spin dynamics in Heisenberg magnets,⁹⁻¹¹ with one exception,¹² have focused on the short-wavelength and/or short-time response of the system. In this paper it is the hydrodynamic region which is of primary interest. We adopt the point of view that our analysis of the ensemble of 4000 spins is an experimental study. We regard our estimates for D_S and D_E as experimental values, which are subject to uncertainties inherent in the experiment. These uncertainties are not unlike the uncertainties associated with the interpretation of the neutron data.

Until recently, studies of one-dimensional magnetic systems had an air of unreality about them. However, the discovery of compounds like $(\text{CH}_3)_4\text{NMnCl}_3$ (TMMC), whose magnetic ions form exchange-coupled chains has made one a respectable dimension for experimentalists and theorists alike.^{13,14} Although our results are for classical spins they are quantitatively correct in the quantum case for $S \gg \frac{1}{2}$, provided the usual replacement, $S^2 - S(S+1)$, is made.

The remainder of the paper is divided into three parts. In Sec. II we discuss the preparation of the array, the solutions to the equations of motion, and the determination of the correlation functions. Our values for D_S and D_E are presented in Sec. III. In Sec. IV we discuss our results. We also make comparisons between our results and the predictions of various theories.

II. EXPERIMENTAL METHOD

The computer experiments consist of two parts, (1) preparation of the equilibrium array, and (2) solution of the equations of motion. The information obtained by the above procedures allows the determination of various correlation functions and dynamical quantities of interest. Since the calculations reported here were undertaken with the aim of inferring spin- and energy-diffusion constants, most of the dynamical quantities extracted were tailored to that goal.

Preparation of an equilibrium array of spins for the one-dimensional Heisenberg magnets is fairly simple given the conditional probability distribution for spin \vec{S}_2 given \vec{S}_1 ,

$$P(\vec{S}_2 | \vec{S}_1) \propto e^{\beta J \vec{S}_2 \cdot \vec{S}_1}, \quad (2.1)$$

where $\beta = 1/k_B T$. Our system consists of 4000 spins represented by three-dimensional unit vectors, each described by three Cartesian components. The first spin is arbitrarily chosen to lie along the x axis. Each successive spin is oriented relative to the previous one by choosing a polar angle and an azimuthal angle distributed appropriately according to the temperature. If α is a random number between 0 and 1, the appropriately distributed polar angle is given by¹¹

$$\mu = \vec{S}_i \cdot \vec{S}_{i+1} = (1/\beta J) \ln[e^{-\beta J} + 2\alpha \sinh \beta J]. \quad (2.2)$$

The azimuth is chosen to be distributed uniformly between 0 and 2π . For the special case of infinite temperature the initialization procedure may be greatly simplified, since the spins are randomly oriented.

As a check on the array prepared in the above fashion, the internal energy of the array may be compared with the exact internal energy.¹⁵ Typical arrays had energies within 1% of the exact values.

The temporal evolution of the equilibrium array is followed by numerically integrating the equations of motion (1.4). The method for doing this is identical to that used in earlier computer experiments on three-dimensional systems by Watson, Blume, and Vineyard.¹⁰ Several internal checks ensure that satisfactory solutions are obtained for times as long as $\tau = tJ = 10$. (We refer to the dimensionless parameter τ as a precession time.) Both the internal energy and magnetization, defined as

$$E = -\frac{J}{N} \sum_{i=1}^{N-1} \vec{S}_i \cdot \vec{S}_{i+1} - \frac{J}{N} \vec{S}_N \cdot \vec{S}_1, \quad (2.3)$$

$$\vec{M} = \frac{1}{N} \sum_{i=1}^N \vec{S}_i, \quad (2.4)$$

are constants of the motion. These quantities, calculated as a function of time, remained constant to within a few percent.

Time-dependent spin and energy correlation functions are calculated at selected intervals of time and averaged over the array of spins. The particular correlation functions derived from the present experiments are the spin and energy self-correlation functions, defined as

$$\langle S(0)S(t) \rangle = \frac{1}{3(N-1)} \sum_{i=1}^{N-1} [S_i^x(0)S_i^x(t) + S_i^y(0)S_i^y(t) + S_i^z(0)S_i^z(t)], \quad (2.5)$$

$$\langle E(0)E(t) \rangle = \frac{1}{N-1} \sum_{i=1}^{N-1} E_i(0)E_i(t), \quad (2.6)$$

where

$$E_i(t) = \frac{1}{2}[\vec{S}_i(t) \cdot \vec{S}_{i+1}(t) + \vec{S}_i(t) \cdot \vec{S}_{i-1}(t)],$$

and the wave-vector-dependent correlation functions which are the spatial Fourier transforms of the r th-neighbor correlation functions. These are given by

$$\langle S(-q, 0)S(q, t) \rangle = \sum_r \cos qr \langle S_{i+r}(0)S_i(t) \rangle, \quad (2.7)$$

$$\langle E(-q, 0)E(q, t) \rangle = \sum_r \cos qr \langle E_{i+r}(0)E_i(t) \rangle. \quad (2.8)$$

In practice, the spatial correlations between distant neighbors are very small, so that the summation over r may be truncated at values ranging from 15 to 50, depending on the temperature. These values were chosen so as to minimize the variation of the zero-wave-vector correlation functions over the interval $0 \leq \tau \leq 10$. Other correlation functions for this system may be constructed in a similar fashion.

The experiments were performed on the Brookhaven CDC-6600 computer. Each run required between 30 and 45 min of computing time, depending on the length of the time evolution and the number of wave vectors q at which the correlation functions were computed.

III. RESULTS

The experimentally determined correlation functions are subject to uncertainties resulting from the finite size of the system and from round-off error in the solution of the equations of motion. In the case of the q -dependent functions, an additional error is introduced in the Fourier-transformation procedure. In an effort to minimize these uncertainties as much as possible, the experiments were repeated with different starting arrays. The results for several choices of array (usually six) were averaged together.

Since our interest here was in spin and energy diffusion, most of our attention was concentrated on the small-wave-vector region where this behavior is most clearly manifested. The major part

of the analysis was carried out with $q = \pi/8$, $\pi/8\sqrt{2}$, and $\pi/16$. Experiments were performed at infinite temperature and at two finite temperatures, $k_B T = 0.5|J|$ and $1.0|J|$.

A. Infinite-temperature results

The experimental wave-vector-dependent correlation functions at infinite temperature for the three choices of wave vector are displayed in Fig. 1. Shown here are the individual results for six different starting arrays as well as the average of the six runs. Figure 2 shows the same results for the energy correlation functions. The most notable feature of this comparison is the fluctuation in the initial value of the correlation functions for different equilibrium arrays. For the energy case it is possible to estimate the expected magnitude of these fluctuations. Heller¹⁶ has shown that the fractional rms fluctuation of the zero-time energy

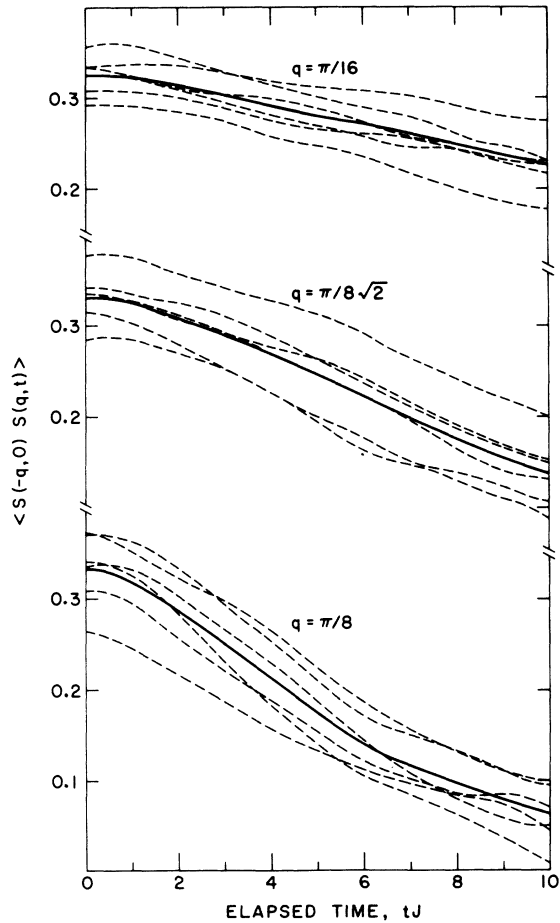


FIG. 1. The wave-vector-dependent spin correlation functions for three choices of wave vector q at infinite temperature. The dashed curves are the results for six different starting arrays. The solid line is the average of the six runs.

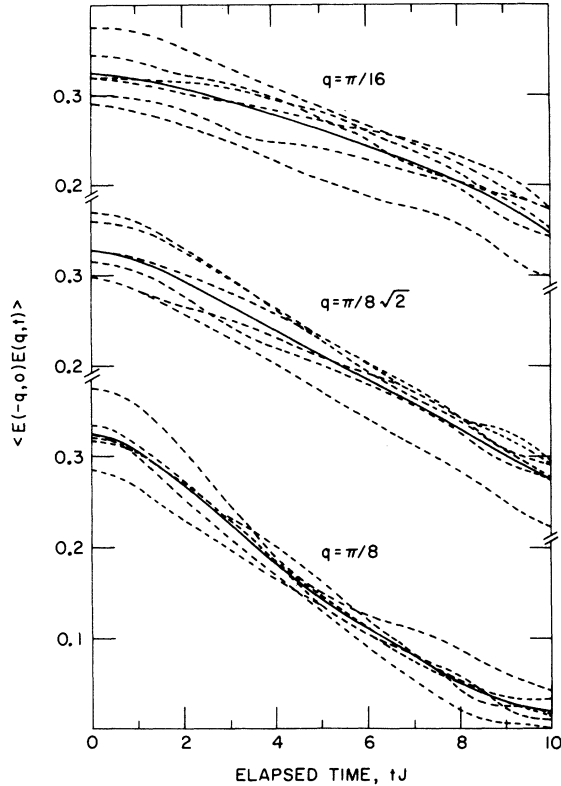


FIG. 2. The wave-vector-dependent energy correlation functions for three choices of q at infinite temperature. The dashed curves are the results for six different arrays; the solid line is their average.

correlation function is given approximately by

$$\delta\mathcal{E} \approx \sqrt{2} \left[\frac{R}{N} - \frac{1}{2N} + \frac{1}{2N} \frac{\sin(2R+1)q}{\sin q} \right]^{1/2},$$

where N is the number of spins in the chain and R is the cutoff of the spatial Fourier transformation. For the conditions of the experiments, namely, $N = 4000$ and $R = 15$, we find $\delta\mathcal{E} = 0.087$. Using the experimental results for 6 different arrays, at $q = \pi/8$, the comparable quantity (the square root of the variance divided by the mean) is 0.082. In other words, the magnitude of the observed fluctuations is precisely what is expected, and is the result of the finite size of the arrays.

The self-correlation functions are somewhat more accurate, since they do not involve a Fourier transformation. However, these were also averaged together for the six separate runs. The resulting spin and energy self-correlation functions at infinite temperature are shown (on a logarithmic scale) in Fig. 3.

The short-time behavior of all the correlation functions may be checked by comparing against a short-time expansion which involves the first few

frequency moments of the Fourier time transform of the correlation functions. The moments are defined (for the spin case) by

$$\langle \omega^n \rangle_S = \frac{\int_{-\infty}^{\infty} \omega^n \mathfrak{s}(q, \omega) d\omega}{\int_{-\infty}^{\infty} \mathfrak{s}(q, \omega) d\omega}, \quad (3.1)$$

where

$$\mathfrak{s}(q, \omega) = \int_{-\infty}^{\infty} e^{i\omega t} \langle S(-q, 0)S(q, t) \rangle dt. \quad (3.2)$$

Equation (3.1) is equivalent to

$$\langle \omega^n \rangle_S = (i)^n \frac{\partial^n}{\partial t^n} \left(\frac{\langle S(-q, 0)S(q, t) \rangle}{\langle S(-q, 0)S(q, 0) \rangle} \right) \Big|_{t=0}. \quad (3.3)$$

In the infinite-temperature limit the second and fourth moments of the spin correlation function for classical spins of unit magnitude are, without approximation¹⁷

$$\langle \omega^2 \rangle_S = \frac{4}{3} J^2 (1 - \cos q), \quad (3.4)$$

$$\langle \omega^4 \rangle_S = \frac{8}{9} J^4 (5 - 3\cos q)(1 - \cos q). \quad (3.5)$$

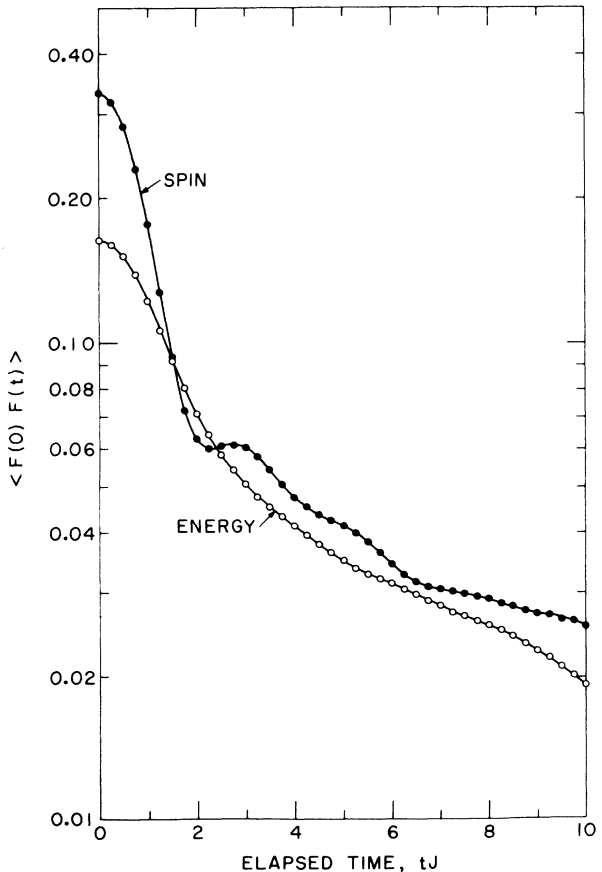


FIG. 3. The infinite-temperature spin and energy self-correlation functions

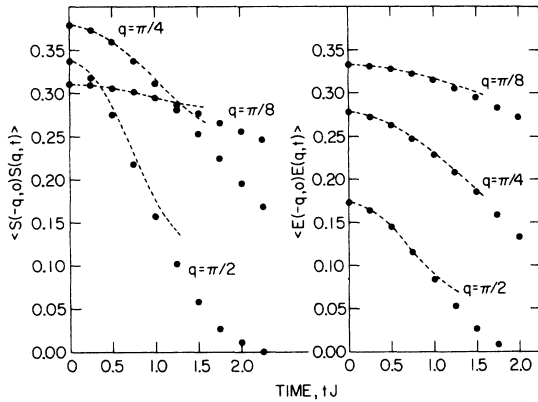


FIG. 4. Short-time behavior of the spin and energy correlation functions for several wave vectors. The points are the results of the computer experiments. The dashed line is the short-time expansion, Eq. (3.8).

Similar results have been found for the energy case, where we have¹²

$$\langle \omega^2 \rangle_E = \frac{4}{3} J^2 (1 - \cos q), \tag{3.6}$$

$$\langle \omega^4 \rangle_E = \frac{8}{9} J^4 (5 - 4 \cos q)(1 - \cos q). \tag{3.7}$$

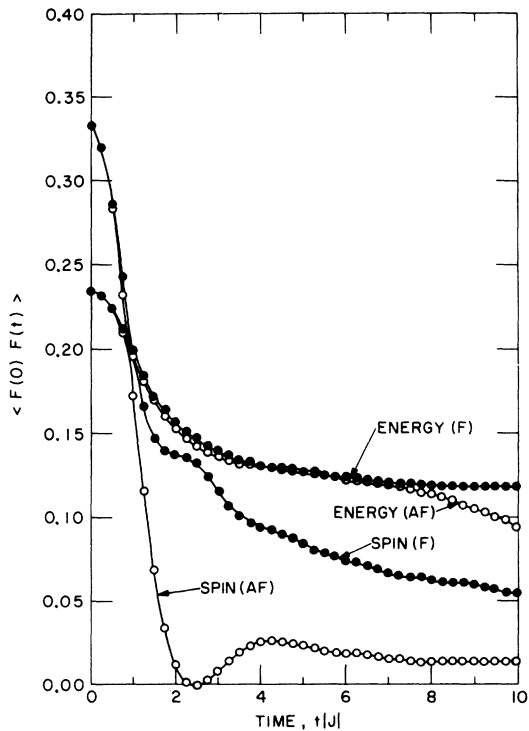


FIG. 5. The spin and energy self-correlation functions at $k_B T = 1.0 |J|$. The solid points are for ferromagnetic coupling, $J > 0$; the open circles are for the antiferromagnet, $J < 0$.

The short-time expansion leads to the following form which is valid for either the spin or energy

$$\frac{\langle F(-q, 0)F(q, t) \rangle}{\langle F(-q, 0)F(q, 0) \rangle} = 1 - \frac{1}{2} \langle \omega^2 \rangle t^2 + \frac{1}{24} \langle \omega^4 \rangle t^4. \tag{3.8}$$

Including the fourth moment, we found very good agreement with the experimental functions up to about one precession time ($\tau = 1$). This comparison is shown in Fig. 4 for several choices of wave vector.

The fact that the arrays we have studied are finite in size has two effects. First, there is the statistical accuracy of the correlation functions due to the finite number of spins used, and second, there could be an effect on the diffusion constant as a result of the finiteness of the chains. The statistical-fluctuation part is reasonably well understood and is proportional $1/\sqrt{N}$. Indeed, we have made studies for chains of 1000 spins and these show a statistical spread a factor of 2 larger. Moreover, by averaging about twice as many runs we obtained an average spin correlation function

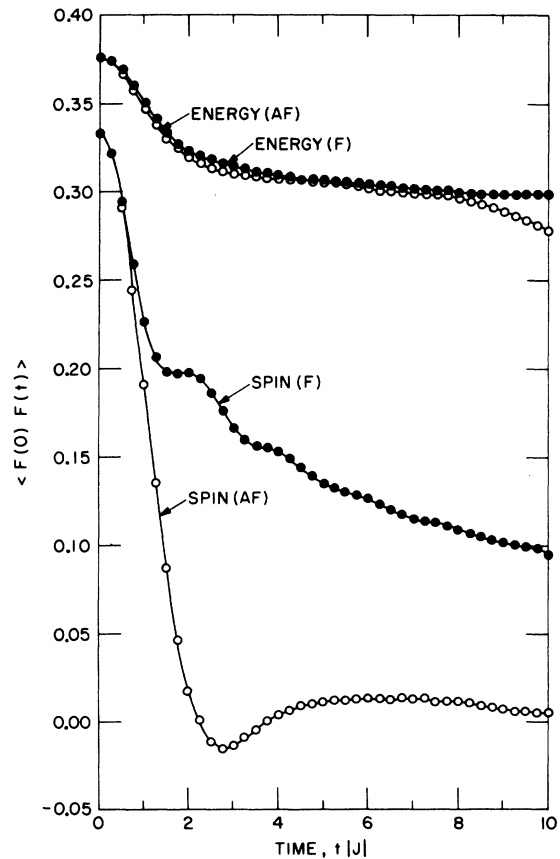


FIG. 6. The spin and energy self-correlation functions at $k_B T = 0.5 |J|$. The solid points are for $J > 0$; the open circles are for $J < 0$.

identical to that determined from a 4000-spin array.

The second effect is more difficult to quantify accurately, but some qualitative observations can be made. Clearly, size effects will be important in two cases: when the correlation length is of the order of the chain size, or for times such that an excitation has a chance to propagate around the chain. Hence, size effects should be important at low temperatures such that $\xi(T) \sim L$, where ξ is the correlation length, and at times t for which $vt \sim L$, where v is a characteristic velocity of propagation of excitations. For $L = 4000$, the temperature T at which $\xi(T) \sim L$ is $T \sim J/4000$, since $\xi \sim J/T$ for low T . This is of course a much lower temperature than any studied. Similarly, the time argument shows that physical size effects should occur for times $t \sim L/V \sim L/J$, since the largest-velocity spin waves in an antiferromagnet have $v = J$. Our calculations extend at most to a time $t = 10/J$, so that, for practical purposes, only statistical fluctuations are significant, and these are well understood.

B. Finite temperatures

The spin correlation functions were also studied at two finite temperatures $k_B T = 0.5|J|$ and $k_B T = 1.0|J|$, for both ferromagnetic ($J > 0$) and antiferromagnetic ($J < 0$) coupling. At infinite temperature there is no distinction between the two types of coupling. A study of the q -dependent energy correlations at finite temperatures was not successful because of the large numerical fluctuations from run to run. The results for the finite-temperature self-correlation functions are given in

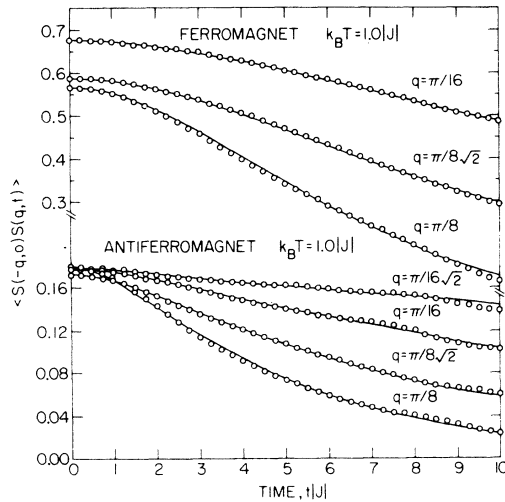


FIG. 7. The experimental data (circles) and the least-squares fits (lines) to the interpolation model for a temperature of $k_B T = 1.0|J|$.

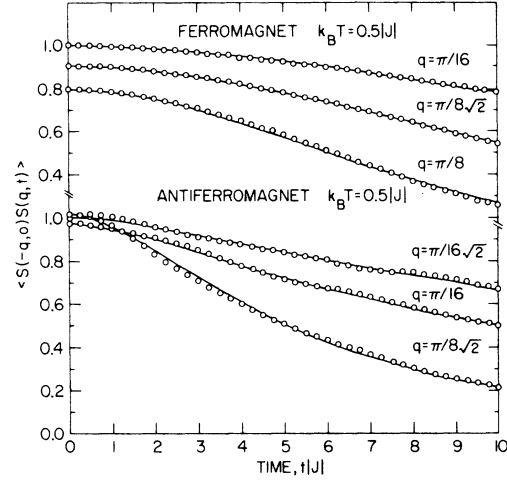


FIG. 8. Spin correlation functions and least-squares fits for a temperature of $k_B T = 0.5|J|$.

Figs. 5 and 6. The q -dependent results are shown in Figs. 7 and 8.

The second and fourth moments at finite temperatures have been given by several authors.^{18,19} For classical spins of unit magnitude they reduce to

$$\langle \omega^2 \rangle_S = \frac{4J}{\beta} \frac{u}{1-u^2} (1 - \cos q)(1 + u^2 - 2u \cos q), \quad (3.9)$$

$$\begin{aligned} \langle \omega^4 \rangle_S = & \frac{2}{3} J^2 \langle \omega^2 \rangle_S^2 \{ 5 - 3 \cos q + (1 - 3u/\beta J) \\ & \times (1 - 3 \cos q + 3/u) - u[6 \cos q - (3 - 3u/\beta J) \\ & \times \cos 2q] \}, \end{aligned} \quad (3.10)$$

where

$$u = \coth \beta J - 1/\beta J.$$

As with the infinite-temperature case, good agreement is found between the experimental results and a short-time expansion to $O(t^4)$ up to about one precision time.

C. Method of analysis

In the small-wave-vector (or long-wavelength) region, at sufficiently long times, the correlation functions are expected to show diffusive behavior, as noted in Sec. I, and should be described by the asymptotic form

$$\langle F(-q, 0)F(q, t) \rangle \sim e^{-Dq^2 t}, \quad (3.11)$$

where D is the diffusion constant. From the preceding discussion we also know that at short times they must behave as $e^{-\langle \omega^2 \rangle t^2 / 2}$. One may construct a variety of models which interpolate between these limits. We have chosen one of the simplest. It is

$$C(q, t) \equiv \frac{\langle F(-q, 0)F(q, t) \rangle}{\langle F(-q, 0)F(q, 0) \rangle} = \exp\left[-\langle \omega^2 \rangle \int_0^t (t-\tau) f(\tau) d\tau\right], \quad (3.12)$$

so that the diffusion constant may be identified as

$$D = \lim_{q \rightarrow 0} \frac{\langle \omega^2 \rangle}{q^2} \int_0^\infty f(\tau) d\tau, \quad (3.13)$$

where $f(\tau)$ must be a decaying function. Two possible choices are (a) $f(\tau) = e^{-A\tau}$ and (b) $f(\tau) = e^{-A^2\tau^2}$. Evaluating (3.12) for both forms yields

$$(a) \quad C(q, t) = \exp\left\{-\frac{1}{2}\langle \omega^2 \rangle \left[2t/A - 2(1 - e^{-At})/A^2\right]\right\} \quad (3.14)$$

$$(b) \quad C(q, t) = \exp\left\{-\langle \omega^2 \rangle \left[t \int_0^t e^{-A^2u^2} du - (1/2A^2) \times (1 - e^{-A^2t^2})\right]\right\}. \quad (3.15)$$

One may easily demonstrate that both of the above forms have the correct long- and short-time limits. Note that both involve only a single unknown parameter, A , related to the diffusion constant by

$$D = \frac{1}{A} \lim_{q \rightarrow 0} \left(\frac{\langle \omega^2 \rangle}{q^2}\right), \quad (3.16)$$

for Eq. (3.14), and

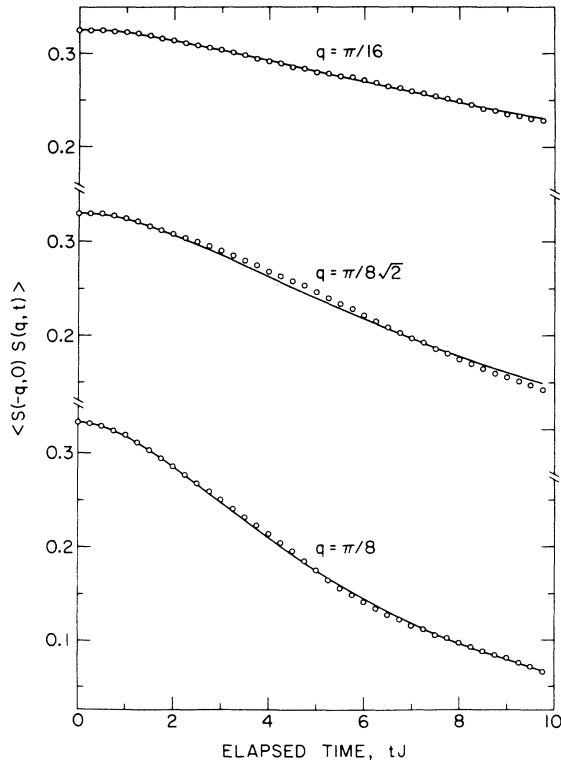


FIG. 9. The spin correlation functions (circles) and the least-squares fits (lines) to the interpolation model [Eq. (3.14)] at infinite temperature.

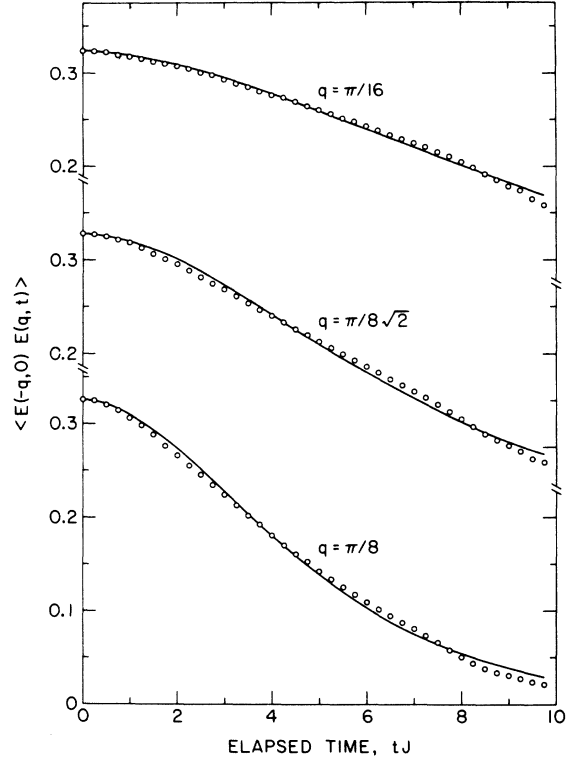


FIG. 10. Energy correlation functions at infinite temperature and least-squares fits.

$$D = \frac{\sqrt{\pi}}{2A} \lim_{q \rightarrow 0} \left(\frac{\langle \omega^2 \rangle}{q^2}\right) \quad (3.17)$$

for (3.15). (The physical significance of A is discussed in Sec. IV.) Both of the above forms were fitted to the experimental data using a least-squares procedure. The two forms give almost

TABLE I. Infinite-temperature diffusion constants.

		D/JSa^2	
		Spin	Energy
Interpolation model ^b	fit to averaged data	1.34 ± 0.02	2.6 ± 0.2
	average of fits to individual runs	1.33 ± 0.10	2.2 ± 0.6
Exponential ^c fit (to tail)		1.33 ± 0.06	2.8 ± 0.7
Best values		1.33 ± 0.10	3 ± 1

^a S denotes the magnitude of the spin; a is the lattice parameter.

^bFit based on Eq. (3.14).

^cFit based on Eq. (3.18).

identical results. Form (a) appears to fit slightly better, and the values of the diffusion constants quoted were based on that model. The comparisons between the experimental data and the fits are shown in Figs. 9 and 10 for the spin and energy cases, respectively. For the infinite temperature case we fitted each individual run (that is, for each different array) as well as the averaged data from the six arrays, obtaining essentially identical values. The results are given in Table I. In this table we write D_S and D_E in conventional units of JSa^2 , where S is the magnitude of the spin and a is the lattice parameter.

As a further check we also fitted the long-time region to a simple exponential of the form

$$C(q, t) = Be^{-Dq^2 t} \quad (3.18)$$

For this case there are two unknown parameters, since the zero-time intercept is not fixed. There is also the problem of determining when the diffusive region has been reached. For these reasons the simple form (3.18) is not expected to give results as accurate as the interpolation model procedure. In order to deal with the problem of determining the onset of the diffusive region we adopted the following method. We first fitted the long-time region $8 \leq \tau \leq 10$ and then gradually extended the portion to be included in the fit to shorter and shorter times until it was clear that a simple exponential no longer described the shape. For most cases this cutoff was at $\tau \approx 4$. The diffusion constants obtained from this procedure are also listed in Table I. It is seen that they are in good agreement with those obtained from the interpolation fits.

The values quoted in Table I are averages for the various q values investigated. The error quoted is chosen large enough to include all the values of D obtained at the different wave vectors, and is typically a factor of 2 larger than the standard deviation of an individual least-squares fit.

TABLE II. Spin-diffusion constants at finite temperatures.

Exchange	$D_S/ J Sa^2$	
	Temperature ($k_B T/ J $)	Interpolation model fit ^b
Ferromagnetic ($J > 0$)	1.0	1.50 ± 0.15
	0.5	1.58 ± 0.20
Antiferromagnetic ($J < 0$)	1.0	1.61 ± 0.15
	0.5	2.19 ± 0.20

^a S denotes the magnitude of the spin; a is the lattice parameter.

^bFit based on Eq. (3.14).

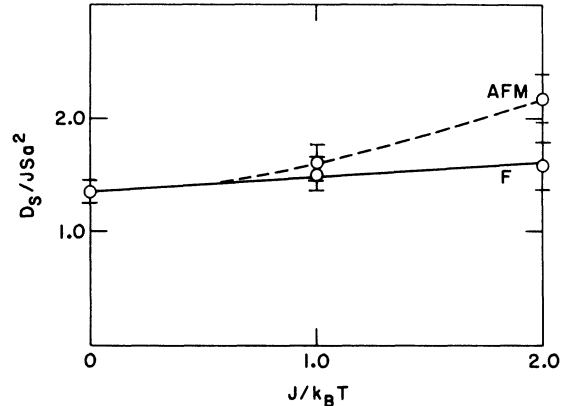


FIG. 11. Temperature dependence of the spin-diffusion constant for ferromagnetic coupling (F), and anti-ferromagnetic coupling (AFM).

The row of "best values" in the table represents what we feel are the most realistic numbers obtainable from the present experiments.

Identical procedures were used to fit the finite-temperature data (Figs. 7 and 8). These results are given in Table II and Fig. 11.²⁰

IV. DISCUSSION

In Secs. III and IV we outlined the numerical analysis of the dynamics of the classical Heisenberg chains. By making use of various fitting procedures we inferred values for the spin- and energy-diffusion constants. In this section we discuss our results and compare the values for D_S and D_E with the predictions of various theories.

Prior to considering the long-wavelength behavior we comment briefly on the spin and energy self-correlation functions, Figs. 3, 5, and 6. As mentioned, these functions are more accurately determined than either $\langle S(-q, 0)S(q, t) \rangle$ or $\langle E(-q, 0) \times E(q, t) \rangle$. This is evident in Fig. 3, where the values at $t=0$, 0.333417, and 0.164405 are very close to the theoretical values $\frac{1}{2}$ and $\frac{1}{4}$. As functions of time both $\langle S(0)S(t) \rangle$ and $\langle E(0)E(t) \rangle$ decay rapidly, with the spin function showing somewhat more structure. However, even at $tJ=10$ neither function has the asymptotic form $Ct^{-1/2}$ characterizing diffusive decay. This is not surprising in view of our results (see below) that the diffusive behavior in $\langle S(-q, 0)S(q, t) \rangle$ and $\langle E(-q, 0)E(q, t) \rangle$ is limited to $q \leq \pi/10$ and $Jt > 4$. At finite temperatures the self-correlation functions decay less rapidly. The significantly slower decay in the energy function is attributed to the fact that at finite temperatures $\langle E \rangle \neq 0$. As a consequence we expect that $\langle E(0)E(t) \rangle \rightarrow \langle E \rangle^2$ as $t \rightarrow \infty$. With our definition of E , Eq. (2.6), and Fisher's¹⁵ results for $\langle E \rangle$, we obtain the values

$\langle E \rangle^2 = 0.098$ and 0.214 for $k_B T = 1.0|J|$ and $0.5|J|$, respectively.

As noted in Sec. I the hydrodynamic equations are expected to characterize only the low-frequency-long-wavelength response of the system. In addition to yielding values for the transport coefficients, our studies also provide information about the boundaries of the hydrodynamic region. At infinite temperature we found that diffusive behavior was limited to wave vectors, $q \leq \pi/10$. For larger values of q , the correlation functions could not be fitted to a simple exponential form at long times. It should be noted that the range of q over which diffusive behavior was observed corresponded quite closely to the range in which the second moment is proportional to q^2 . At finite temperatures it is expected that the diffusive regime is further restricted by the condition $q \leq \kappa$, where κ is the inverse correlation length. Unfortunately we were not able to carry out sufficiently accurate analyses at low enough temperatures to verify this prediction.

It was also pointed out that the time dependence of the correlation functions was accurately reproduced by the first three terms in the moment expansion for $0 \leq \tau \leq 1$. On the other hand, the simple exponential form, $e^{-D\tau}$, was appropriate only for $\tau > 4$. From this we conclude that the time to reach local thermal equilibrium is on the order of 2–4 precession times. As a consequence the frequency boundary of the hydrodynamic region at infinite temperature is approximately $\frac{1}{4}J$.

Our discussion of the magnitude of D_S and D_E begins with the formal expressions for the spin and energy diffusion constants, which take the form of time integrals over appropriate current-current correlation functions.^{1,4,21,22} We have

$$D_{S,E} = \lim_{\omega \rightarrow 0} \frac{1}{2} R_{S,E}^{-1} \int_{-\infty}^{\infty} e^{i\omega t} \langle \{j_{S,E}(0), j_{S,E}(t)\} \rangle dt, \quad (4.1)$$

where $\{A, B\} = \frac{1}{2}(AB + BA)$. The symbol R_S denotes the product $k_B T \chi_T$, where χ_T is the isothermal susceptibility in units of $g^2 \mu_B^2$. R_E is equal to $k_B T^2 C_H$, where C_H is the specific heat. The symbols j_S and j_E denote the spin and energy currents, respectively, and are determined by the continuity equations

$$\frac{\partial S(q, t)}{\partial t} + iqj_S = 0, \quad (4.2)$$

$$\frac{\partial E(q, t)}{\partial t} + iqj_E = 0. \quad (4.3)$$

For one-dimensional Heisenberg magnets with nearest-neighbor interactions j_S and j_E take the form

$$j_S = J \sum_n S_y^n (S_x^{n+1} - S_x^{n-1}), \quad (z \text{ component}), \quad (4.4)$$

$$j_E = J^2 \sum_n \tilde{S}^n \cdot (\tilde{S}^{n+1} \times \tilde{S}^{n-1}). \quad (4.5)$$

In the case of classical systems (or quantum systems at infinite temperatures) the ratio $\langle j_{S,E}(0) \times j_{S,E}(0) \rangle / R_{S,E}$ is equal to $\lim_{q \rightarrow 0} (\langle \omega^2 \rangle_{S,E} / q^2)$, where $\langle \omega^2 \rangle_{S,E}$ is the second moment, as defined in Sec. II. This has the consequence that (4.1) can be rewritten in the form

$$D_{S,E} = \lim_{q \rightarrow 0} \left(\frac{\langle \omega^2 \rangle_{S,E}}{q^2} \right) \int_0^{\infty} \frac{\langle j_{S,E}(0) j_{S,E}(t) \rangle}{\langle j_{S,E}(0) j_{S,E}(0) \rangle} dt, \quad (4.6)$$

from which it is evident that the parameter A , introduced in Sec. III is a measure of the decay rate of the current-current correlation function.

Following the approach of Ref. 12 we first attempted to infer the diffusion constant by calculating the current-current correlation functions. Results from a single run are shown in Fig. 12. The rapid falloff in the correlation is apparent. However, the structure in the slowly decaying tail was not reproducible from run to run. In light of this, it was felt that a numerical evaluation of the integral in (4.1) would lead to large errors in the estimates of the diffusion constants. As a consequence this approach was abandoned in favor of a direct analysis of the spin and energy correlation functions.²³

From Table I it is seen that D_E is approximately a factor of 2 larger than D_S . Since $\langle \omega^2 \rangle_S$ is equal to $\langle \omega^2 \rangle_E$ at infinite temperature we conclude that the correlations in the thermal current decay more slowly than the correlations in the spin cur-

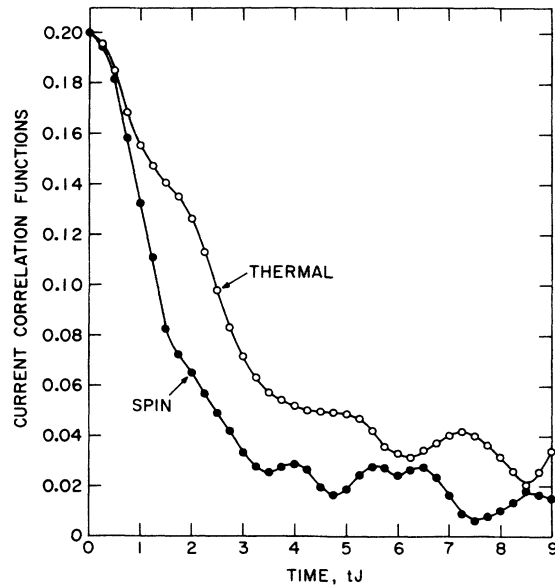


FIG. 12. Spin and thermal (or energy) current auto-correlation functions at infinite temperature.

rent. Because j_E is a constant of the motion for the spin- $\frac{1}{2}$ chain with nearest-neighbor interactions,^{24,25} we are led to conjecture that the difference in the decay rates of the energy and spin current-current correlation functions becomes more pronounced as one passes from classical spins to quantum spins with small values of S .

The data in Table II show that the spin-diffusion constants are nearly temperature independent in the interval $\infty > k_B T > |J|$, but begin to vary at lower temperatures. These results are to be compared with the ratios of the second moments, $\lim_{q \rightarrow 0} \langle \omega^2 \rangle_S(T) / \langle \omega^2 \rangle_S(\infty)$. For ferromagnets, this ratio is 0.49 and 0.24 for $k_B T = J$ and $0.5J$, respectively. In the case of antiferromagnets, the corresponding values are 1.80 and 2.68 for $k_B T = |J|$ and $0.5|J|$. In light of Eq. (4.6), we conclude that the spin-current correlation function in the ferromagnetic chain decays more slowly at finite temperatures than in the infinite-temperature limit. In the antiferromagnetic chain, there is an apparent speeding up of the decay for $k_B T \geq 0.5|J|$ since the increase in D_S is less than expected from the temperature dependence of the second moment alone. In the large region between $J/k_B T = 0$ and 1 the diffusion constant seems to be temperature independent or slowly varying. However, since we have determined so few points we cannot exclude the possibility of some other behavior in that region. Indeed, Reiter has suggested³² that to first order in $J/k_B T$ the slopes of the diffusion constants ought to be of opposite sign for the ferromagnet and antiferromagnet in the high-temperature region. The accuracy of our values and the scarcity of points in the high-temperature region do not permit us to comment on this prediction.

Because of the large fluctuations from run to run, it was not possible to obtain consistent values of D_S for $k_B T$ less than $0.5|J|$. As a consequence, we were unable to test a recent theoretical prediction that the spin-diffusion constant of the classical antiferromagnetic chain diverges as T^{-1} as $T \rightarrow 0$, while D_S for the ferromagnetic chain remains finite in the same limit.²⁶

Theoretical calculations of D_S and D_E generally have followed one of two approaches. The first of these involves a short-time expansion of $\langle j_{S,E}(0) \times j_{S,E}(t) \rangle$. We have

$$\frac{\langle j_{S,E}(0) j_{S,E}(t) \rangle}{\langle j_{S,E}(0) j_{S,E}(0) \rangle} = 1 - \frac{1}{2} \frac{\langle \omega^4 \rangle_{S,E}}{\langle \omega^2 \rangle_{S,E}} t^2 + O(t^4), \quad (4.7)$$

where it is understood that the ratio $\langle \omega^4 \rangle_{S,E} / \langle \omega^2 \rangle_{S,E}$ is to be evaluated in the $q \rightarrow 0$ limit. Keeping only the first two terms in the expansion, and making the usual approximation, $1 - a^2 t^2 \approx e^{-a^2 t^2}$, leads to the result²¹

$$D = \left(\frac{\pi}{2} \right)^{1/2} \lim_{q \rightarrow 0} \left(\frac{\langle \omega^2 \rangle}{q^2} \right) \left(\frac{\langle \omega^4 \rangle}{\langle \omega^2 \rangle} \right)^{1/2}. \quad (4.8)$$

With the values for the moments given previously it is found

$$D_S = 0.73 JSa^2, \quad (4.9)$$

$$D_E = 1.03 JSa^2 \quad (4.10)$$

in the high-temperature limit.

It is apparent that keeping only the first two terms in the short-time expansion leads to spin- and energy-diffusion constants that are smaller than the measured values by factors of 2 and 3, respectively. The source of the error is in the time dependence of $\langle j_{S,E}(0) j_{S,E}(t) \rangle$. The postulated form,

$$\langle j_{S,E}(0) j_{S,E}(t) \rangle = \exp \left(- \frac{1}{2} \frac{\langle \omega^4 \rangle_{S,E}}{\langle \omega^2 \rangle_{S,E}} t^2 \right),$$

underestimates the rate of decay.

In the case of spin diffusion, attempts have been made to go beyond the simple Gaussian approximation.^{27,28} For the classical chain the low-order corrections are about 30%, with the consequence that D_S is estimated to be on the order of $0.9 JSa^2$. This result is to be compared with our measured value $(1.33 \pm 0.1) JSa^2$. It should be noted that the shortcomings of small-time expansion for Heisenberg magnets at infinite temperature appears to be limited to one dimension. In higher dimensions the corrections to the Gaussian approximation are small,^{27,28} and in the case of three dimensions the discrepancy between D_S , calculated from (4.8), (with moments appropriate to finite spin and temperature) and the room-temperature value for the spin-diffusion constant in RbMnF_3 is less than 5%.²⁹ Because of the greater complexity of the moment calculations, short time expansions of the thermal-current correlation functions have not gone beyond the first two terms. However, it is doubtful that the disagreement between 1 and 3 would be removed by including only a few of the higher moments.

In the other approach to the calculation of the spin-diffusion constants the local-spin operators appearing in the definition of j_S and j_E are expanded in terms of their Fourier components $\tilde{S}(q)$. The multispin-current correlation functions are then factorized into products of two-spin functions $\langle S(-q, 0) S(q, t) \rangle$, a procedure often referred to as the independent-mode approximation. Since $\langle S(-q, 0) S(q, t) \rangle$ depends on D_S for small q the calculation of the spin-diffusion constant by this method becomes self-consistent.³⁰ Early calculations of D_S and D_E following this approach, which used primitive two-spin functions, led to the result $D_S = 0.58 JSa^2$ and $D_E = 0.23 JSa^2$, in one dimension

at infinite temperature.³¹ In their paper, McLean and Blume reported a calculation of D_S in the independent-mode approximation using what appear to be the most accurate of the currently available theoretically determined two-spin functions.¹⁹ At infinite temperature they obtain the value $D_S = 1.38 J S a^2$, in excellent agreement with our results. However, in view of the uncertainties associated with the factorization, it is not clear at this time whether the agreement is fortuitous. For this reason it is important to carry out similar calculations in a formalism which incorporates the interaction between the modes.³² In line with this it would seem to be worthwhile to repeat the calculation of D_E in the independent-mode approximation using realistic two-spin functions. In this case the factorization reduces a six-spin function to a product of three two-spin functions and hence is a particularly sensitive test of the decoupling. In the Appendix we consider the independent-mode

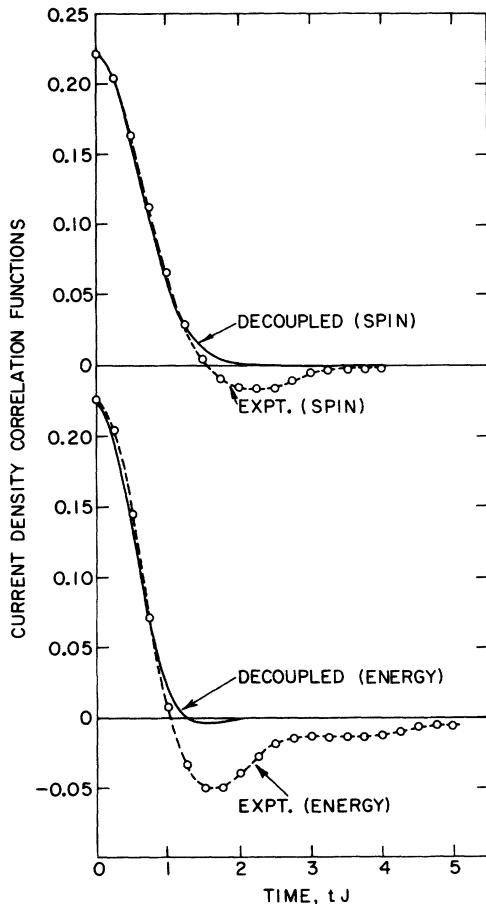


FIG. 13. Comparison of the spin and energy current density correlation functions, and the corresponding functions calculated using the independent-mode approximation.

approximation in the slightly different context of the determination of the self-correlation functions of the spin and energy current densities. There it is shown that the approximation is accurate out to one precession time. Beyond that point it begins to break down, with the greatest discrepancy associated with the energy functions.

In summary, the goal of the study reported in this paper was to probe the dynamics of the classical Heisenberg chain in the hydrodynamic region. By fitting appropriate correlation functions, values were inferred for the spin- and energy-diffusion constants. Strictly speaking, our values for D_S and D_E were obtained from a study of the decay of $\langle S(-q, 0)S(q, t) \rangle$ and $\langle E(-q, 0)E(q, t) \rangle$ for a chain of 4000 spins. The calculations were carried out over the interval $0 \leq \tau \leq 10$ and for wave vectors between $\pi/8$ and $\pi/16$. As a consequence it is possible, although we believe not likely, that our values for the diffusion constant are not truly representative of the hydrodynamic region. To settle this question would necessitate calculations of significantly larger arrays with smaller wave vectors and extending over longer time intervals. Such calculations appear to be beyond the capability of present day computers, but may become feasible in the future.

ACKNOWLEDGMENTS

It is a pleasure to thank P. Heller for providing his unpublished results on the fluctuations and for his continued interest in this problem, and R. E. Watson, G. H. Vineyard, and G. Reiter for helpful discussions of unpublished results.

APPENDIX

In this Appendix we assess the independent-mode approximation as applied to the evaluation of the self-correlation function of the spin and energy current densities. These functions, denoted by g_S and g_E are expressed as

$$g_S(t) = \langle S_y^n (S_x^{n+1} - S_x^{n-1})(t) S_y^n (S_x^{n+1} - S_x^{n-1})(0) \rangle, \quad (\text{A1})$$

$$g_E(t) = \langle \vec{S}^n \cdot \vec{S}^{n+1} \times \vec{S}^{n-1}(t) \vec{S}^n \cdot (\vec{S}^{n+1} \times \vec{S}^{n-1})(0) \rangle. \quad (\text{A2})$$

From Eqs. (4.4)–(4.6) it is seen that the $g_{S,E}(t)$ are the dominant terms in $\langle j_{S,E}(0)j_{S,E}(t) \rangle$ for small times. In the independent-mode approximation g_S and g_E are given by

$$g_S = 2f_0(f_0 - f_2), \quad (\text{A3})$$

$$g_E = 6(f_0 - f_2)[f_0^2 + f_0 f_2 - 2f_1^2], \quad (\text{A4})$$

where the f_n denote the correlation functions

$$f_n^{(t)} = \langle S_i^z(0)S_{i+n}^z(t) \rangle.$$

We have evaluated (A1)–(A4) at infinite temper-

ature using computer-generated f_n . The results are shown in Fig. 13. It is apparent that the approximation is reasonably accurate out to about one precession time. Beyond that point the factorization begins to break down, with the energy functions showing the greatest discrepancy. The agreement between the approximate and exact curves at $t=0$ is a direct consequence of the condition of infinite temperature and the fact that both current densities involve combinations of terms,

each of which is of the form $(S_i^x)^l (S_j^y)^m (S_k^z)^n$ with $0 \leq l, m, n \leq 1$. It should be kept in mind that our findings are not necessarily representative of the accuracy of the independent-mode approximation as applied to the (total) spin- and energy-current correlation functions at finite or even at infinite temperature. These functions incorporate correlations between densities at different points which may not be as accurately reproduced in factored form.

*Work performed under the auspices of the U. S. Atomic Energy Commission.

†Supported by the National Science Foundation.

¹J. S. Guggenheim Fellow, 1972–1973; permanent address, Physics Dept., University of Wisconsin, Madison, Wis.

²L. P. Kadanoff and P. C. Martin, *Ann. Phys. (N. Y.)* **24**, 419 (1963).

³L. D. Landau and E. M. Lifshitz, *Fluid Mechanics* (Addison-Wesley, Reading, Mass., 1959).

⁴S. Chapman and T. G. Cowling, *The Mathematical Theory of Non-Uniform Gases*, 3rd ed. (Cambridge U. P., London, 1970).

⁵H. Mori, *Progr. Theor. Phys. (Kyoto)* **33**, 423 (1965).

⁶N. Bloembergen, *Physica (Utr.)* **15**, 386 (1949); see also L. Van Hove, *Phys. Rev.* **95**, 1374 (1954).

⁷B. I. Halperin and P. C. Hohenberg, *Phys. Rev.* **188**, 898 (1969).

⁸C. P. Enz, *Phys. Kondens. Mater.* **12**, 262 (1971).

⁹E. R. Hunt and J. R. Thompson, *Phys. Rev. Lett.* **20**, 249 (1968).

¹⁰C. G. Windsor, *Neutron Inelastic Scattering* (International Atomic Energy Agency, Vienna, 1968), Vol. II, pp. 83–92; *Proc. Phys. Soc. Lond.* **91**, 353 (1967).

¹¹R. E. Watson, M. Blume, and G. H. Vineyard, *Phys. Rev.* **181**, 811 (1969).

¹²M. Blume, R. E. Watson, and G. H. Vineyard, *Bull. Am. Phys. Soc.* **16**, 629 (1971).

¹³D. L. Huber, J. S. Semura, and C. G. Windsor, *Phys. Rev.* **186**, 534 (1969).

¹⁴R. Dingle, M. E. Lines, and S. L. Holt, *Phys. Rev.* **187**, 643 (1969).

¹⁵M. T. Hutchings, G. Shirane, R. J. Birgeneau, and S. L. Holt, *Phys. Rev. B* **5**, 1999 (1972). Because of resolution limitations, it has not been possible to measure the spin-diffusion constant of TMMC by inelastic neutron scattering.

¹⁶M. E. Fisher, *Am. J. Phys.* **32**, 343 (1964).

¹⁷P. Heller (private communication).

¹⁸M. F. Collins and W. Marshall, *Proc. Phys. Soc. Lond.* **92**, 390 (1967).

¹⁹S. W. Lovesey and R. A. Meserve, *Phys. Rev. Lett.* **28**, 614 (1972); *J. Phys. C* **6**, 79 (1973).

²⁰F. B. McLean and M. Blume, *Phys. Rev. B* **7**, 1149 (1973); *Phys. Rev. B* **7**, 5017(E) (1973).

²¹At finite temperatures it is necessary to allow for the wave-vector dependence of the ratio $\langle \omega^2 \rangle / (1 - \cos q)$ in inferring values for D_S from the simple exponential fit. If D_{eff} denotes the parameter obtained by fitting the function $\exp[-D_{\text{eff}} q^2 t]$, then the spin-diffusion constant is given by $D_S = D_{\text{eff}} (1 - u)^2 / [(1 - u)^2 + q^2 u]$, where $u = \coth \beta J - 1/\beta J$.

²²H. Mori and K. Kawasaki, *Progr. Theor. Phys. (Kyoto)* **27**, 529 (1962).

²³K. Kawasaki, *Progr. Theor. Phys. (Kyoto)* **29**, 801 (1963).

²⁴The computer analysis in Ref. 12 led to the value $D_E = (1.7 - 1.9) JSa^2$. It appears that the estimates of the uncertainties in the analysis were unrealistically small.

²⁵D. L. Huber and J. S. Semura, *Phys. Rev.* **182**, 602 (1969).

²⁶D. A. Krueger, *Phys. Rev. B* **3**, 2348 (1971).

²⁷H. Tomita and H. Mashiyama, *Progr. Theor. Phys. (Kyoto)* **48**, 1133 (1972). The same results follow from the one-dimensional version of Kawasaki's self-consistent mode-mode coupling theory [K. Kawasaki, *Progr. Theor. Phys. (Kyoto)* **39**, 285 (1968)].

²⁸D. L. Huber, *Phys. Lett. A* **31**, 267 (1970).

²⁹T. Morita, *Phys. Rev. B* **6**, 3385 (1972).

³⁰A. Tucciarone, J. M. Hastings, and L. M. Corliss, *Phys. Rev. B* **8**, 1103 (1973). Additional evidence for the accuracy of the Gaussian approximation for D_S in three dimensions comes from measurements of the nuclear-spin diffusion constant in ^3He [J. R. Thompson, E. R. Hunt, and H. Meyer, *Phys. Lett. A* **25**, 313 (1967)] where the measured value agrees with the theoretical value to within the experimental error of 10%. In contrast, the Gaussian approximation for D_E in ^3He is approximately a factor of 2 smaller than the measured value [A. G. Redfield and W. N. Yu, *Phys. Rev.* **169**, 443 (1968); *Phys. Rev.* **177**, 1018(E) (1969)].

³¹H. S. Bennett and P. C. Martin, *Phys. Rev.* **138**, A608 (1965).

³²D. L. Huber, *Progr. Theor. Phys. (Kyoto)* **39**, 1170 (1968).

³³G. Reiter (private communication).